Remote Sensing in Ecology and Conservation
Open Access

ORIGINAL RESEARCH

Regional-scale forest restoration effects on ecosystem resiliency to drought: a synthesis of vegetation and moisture trends on Google Earth Engine

Temuulen Sankey[1], Adam Belmonte[1], Richard Massey[1] & Jackson Leonard[2]

[1]School of Informatics, Computing, and Cyber Systems, Northern Arizona University, Flagstaff, AZ, USA
[2]Rocky Mountain Research Station, US Forest Service, Flagstaff, AZ, USA

Keywords
vegetation cover change, time-series data, landsat, forest restoration, drought, Google Earth

Correspondence
Temuulen Sankey, School of Informatics, Computing, and Cyber Systems, Northern Arizona University, Flagstaff, AZ, USA.
Tel: +1-928-523-7098; Fax: +1-928-523-0101; E-mail: Temuulen.Sankey@nau.edu

Editor: Mat Disney
Associate Editor: Dolors Armenteras

Received: 15 July 2020; Revised: 28 September 2020; Accepted: 19 October 2020

doi: 10.1002/rse2.186

Abstract

Large-scale changes in forest structure and ecological function throughout western North America have led to increased frequency, size, and severity of wildfires. The US Forest Service is implementing state-wide forest restoration initiatives to reduce wildfire hazards and improve forest health. We provide a synthesis of pre- and post-treatment forest vegetation and ecosystem moisture trends between 1990 and 2017 in Arizona, the first US state where the initiative has implemented a variety of thinning and burning methods in over 1,200 polygon areas across 3.5 million ha. Using 4,426 Landsat satellite images on Google Earth Engine, we calculated normalized difference moisture index (NDMI), normalized difference water index (NDWI), and normalized difference vegetation index (NDVI) to create dense time-series datasets. The indices and 1990-2017 annual total precipitation dataset were then examined using a Mann–Kendall tau test to identify statistically significant upward and downward trends for each pixel. Our results indicate that much of the study region were experiencing drought conditions prior to restoration treatments and NDVI values were significantly decreasing, especially during the dry spring season. However, both NDMI and NDWI trends indicate that the forest restoration treatments have contributed to increased total ecosystem moisture, while precipitation in the post-treatment period exhibit stable trends. Forest restoration treatments appear to have improved the overall forest health and resiliency to drought, especially during the dry spring season, when forests are most vulnerable to water stress and wildfire risks. Our results of the spatial patterns and long-term trends in these variables can inform the currently ongoing and future restoration treatments to better target the treatment strategy across the southwestern USA. Google Earth Engine enabled our synthesis of these long-term trends over the large region and will enhance our continued monitoring in the coming decade.

Introduction

Global forests provide a critical role in regulating climate, carbon storage, and hydrologic cycling (Foley et al., 2005; Kohl et al., 2015; Trumbore et al., 2015). Forests also provide habitat for plant and animal species (Hidalgo et al., 2015), and many ecosystem services for populations around the world (Miura et al., 2015). Global forests are undergoing large-scale changes and forested areas are declining (Hansen et al., 2013; Keenan et al., 2015) due to fire, drought, insect outbreaks, disease, deforestation, and climate change (Lierop et al., 2015). Land management strategies can substantially alter these trends in forest conditions and increase forest resiliency to disturbance events.

In the southwestern USA, millions of hectares (ha) of ponderosa pine forests have become vulnerable to catastrophic wildfires due to abnormally high tree densities (Allen et al., 2002; Covington et al., 1997), which resulted from previous decades of livestock grazing, fire exclusion, and timber management (Cooper, 1960; Fule et al., 2009; Larson & Churchill, 2012; Savage et al., 1996). Due to the high tree density, approximately 70% of the ponderosa pine forest has been estimated to be at a high risk of bark beetle infestation (USDA, 2013), whereas 34% of the forest is already affected by dwarf mistletoe (USDA, 2013). The dense stands of even-aged, small diameter trees have replaced up to 70% of the ponderosa pine forests, which were historically characterized with naturally open conditions (Covington & Moore, 1994).

The US Forest Service (USFS) recently launched the first and largest restoration effort in the US history known as the Four Forest Restoration Initiative (4FRI) in Arizona to reduce the high tree density (USDA, 2013). Other western US states are launching similar initiatives through the US Forest Service's Collaborative Forest Landscape Restoration Program (Dickinson et al., 2016; Cannon et al., 2018). The 4FRI will conduct forest restoration treatments over 3.5 million ha across Arizona over 20 years with a primary goal to reduce wildfire risk and improve forest health (USDA, 2013). In particular, 4FRI aims to thin and burn the forests to create patches and stands similar to the historic distribution of small groups of trees mixed with open interspaces (Allen et al., 2002; USDA, 2013). The resulting pattern is hoped to improve forest health and functioning and increase total ecosystem moisture retention and water yield (Rich & Gottfried, 1976). The 4FRI activities officially started in 2007 and many treatments have already been accomplished. We provide the first synthesis of the regional forest restoration effort and its impacts on forest health across the state of Arizona, USA. Such comprehensive assessment is critical for other states throughout the United States, who will likely adopt similar restoration initiatives in the coming years and decades (Allen et al., 2002; Dickinson et al., 2016; Cannon et al., 2018), as well as for land managers in Arizona in their adaptive management strategies.

In forested ecosystems, vegetation provides the primary medium that transfers water from the ground to the atmosphere (Asbjornsen et al., 2011; Chapin et al., 2002;). Forest evapotranspiration comprises a large component of the total ecosystem water loss and quantifying this component is critical for forest and water resource management (Asbjornsen et al., 2011; Porporato, 2002;). In arid and semi-arid environments, up to 90% of total annual rainfall can be lost through vegetation evapotranspiration (Huxman et al., 2004). This process is particularly acute in Arizona and the southwestern USA, where rates of evaporation are already high due to high temperatures and low humidity. Furthermore, over the winter months, forest canopies intercept up to 60% of the annual snowfall and can sublimate up to 40% of the snowfall in the canopies (Andreadis et al., 2009). Together, these losses through vegetation canopies can create water deficits in the ecosystem and, in return, reduce total ecosystem productivity (Biederman et al., 2016).

Forest thinning and burning can significantly reduce vegetation canopy cover and density (Belmonte et al., 2019; Briggs et al., 2017; Cannon et al., 2018; Fule et al., 2012; Underhill et al., 2014). As a result, forest evapotranspiration is expected to reduce substantially (Barnes et al., 2016; Dore et al., 2012; Rich & Gottfried, 1976; Zhang et al., 2001; Simonin et al., 2007), which would be expected to lead to greater canopy moisture in the remaining trees and thus greater resiliency to drought. Furthermore, canopy interception of snow and sublimation is similarly reduced (Gottfried & Ffolliott, 1980; Harpold et al., 2014; Sankey et al., 2015), which allows greater snow accumulation on the ground making a greater contribution to the groundwater recharge and water yield (Baker, 1986; Rich & Gottfried, 1976; Simonin et al., 2007). Together, the reduced evapotranspiration, greater canopy moisture in the remaining trees, and improved groundwater recharge would all lead to greater resiliency to drought. These cumulative benefits, however, have not been quantitatively assessed. It is currently unknown whether the regional restoration treatments have had significant ecohydrological impacts in addition to the reduced wildfire risk. We synthesize 4FRI's potential ecohydrological impacts to determine whether the forest restoration activities are increasing total ecosystem moisture (e.g., canopy moisture) and retention and, thereby, improving forest resiliency to drought. In particular, we quantify the extent and spatial patterns of the reduced canopy cover, density, and biomass, subsequently improved canopy moisture resiliency, and identify the specific treatment types that are associated with the improved resiliency, if observed. We use a vegetation index as an approximate estimate of forest canopy vigor, cover, density, and biomass, and we evaluate moisture indices to estimate forest canopy moisture changes and infer improved resiliency.

Monitoring post-treatment forest health and resiliency to drought can be challenging due to subtle vegetation changes that are not immediately apparent in satellite image reflectance (Asner et al., 2004; Sankey, 2012). However, by building a large and dense time-series images from satellite data, we might detect gradual trends in forest health, vigor, and canopy moisture, and thus resiliency. Google Earth Engine (GEE) provides a unique opportunity to synthesize such trends with its large archives of Landsat satellite images and high-performance computing capabilities (Gorelick et al., 2017; Sankey et al., 2018). GEE offers complex analysis capabilities for image classification, change detection, time-series analysis, and vector-based extraction of image statistics (Erickson, 2014; Hancher, 2013; Moore & Hansen, 2011). As a result, GEE has been successfully used in several large-scale studies (Dong et al., 2015; Hansen et al., 2013; Johansen et al., 2015; Massey et al., 2018; Patel et al., 2015; Sankey et al., 2018; Simonetti et al., 2015; Teluguntla et al., 2017).

Our objectives were to: (1) quantify changes in forest condition due to the forest restoration treatments, namely, forest thinning and burning across the state of Arizona, USA, and (2) quantify changes in forest canopy moisture to evaluate whether the forest restoration activities have had potential benefits in forest resiliency to drought. Using the large Landsat image archive on GEE, we synthesize the long-term trends in forest vegetation and forest moisture before and after the forest treatments spanning a total of 27 years between 1990 and 2017. We also integrate the precipitation trends over the 27-year period to assess how restoration treatment impacts interact with precipitation trends at decadal scales, since precipitation plays a critical role in total ecosystem moisture availability and evapotranspiration (Barnes et al., 2016).

Methods

Study Region

Our study focused on four National Forests across the state of Arizona, USA (Figure 1), managed by the US Forest Service: the Kaibab, Coconino, Tonto, and Apache-Sitgreaves (Figure 1). The entire 4FRI boundary includes approximately 3.5 million ha area across an average elevation of 2,000 m ranging between 750 m and 3,850 m. The region encompasses over a million ha of ponderosa pine forests, the largest in the United States, comprising the southernmost ponderosa pine belt in the North American continent. The region experiences cool winters and warm summers. The average precipitation at high elevations is 650 mm, whereas lower elevations receive approximately 450 mm precipitation a year.

We grouped the forest vegetation cover types into the following dominant categories: 1) ponderosa pine (*Pinus ponderosa*), 2) mixed conifers, and 3) pinyon-juniper (*Pinus* spp and *Juniperus* spp). The restoration treatments included areas of controlled burning and mechanical thinning (Table 1) of varying levels of intensity, which we simply grouped into two categories: a) burning, and b) thinning. The primary goal of the thinning and burning treatments is to reduce wildfire risk and improve forest health (USDA, 2013). Specifically, the treatments aim to re-create the historic distribution of small groups of trees mixed with open interspaces, and to promote diversity in tree group and interspace size, shape, and spacing. By emphasizing irregular forest patch sizes, expansion of interspace, and substantial reductions in small understory trees, the treatments ultimately aim to create healthy overstory vegetation and understory regeneration.

Our study also summarizes and focuses on two primary temporal periods: 1) pre-treatment period, which spans 1990-2006, prior to 4FRI restoration activities started, and 2) post-treatment period between 2007 and 2017. The beginning of the post-treatment period varied slightly among the individual treatment polygons, as the exact treatment dates varied per polygon, which we considered and carefully differentiated in our analysis. The treatment polygons, treatment dates, and the treatment descriptions were acquired as shapefiles from the US Forest Service, who records and reports the 4FRI activities annually.

Datasets

We first used the gridded surface meteorological dataset GRIDMET (Abatzoglou, 2012) available on GEE, which provides daily surface temperature, wind, humidity, precipitation, and radiation data in 4 km cells across the contiguous USA since 1979. Of this dataset, we extracted the daily precipitation data between 1990 and 2017 and calculated the total annual precipitation in 4 km cells for every year over the 1990-2017 time period using the reducer and statistical summary tools available in GEE. While the GRIDMET temperature datasets have median correlations of 0.87–0.95 with independent validation datasets, the precipitation datasets have correlations of approximately 0.85 with validation datasets with an average bias of 5% (Abatzoglou, 2012). We created two separate layer stacks of annual total precipitation for 1990-2006 and 2007-2017 time periods using a layer stack function along with an image collection tool. The 1990-2006 time-period layer stack, therefore, included 17 raster bands, whereas the 2007-2017 layer stack had 11 bands of total annual precipitation. We created these two-layer stacks to separately examine temporal trends in the total annual precipitation within each time-period to first determine if statistically significant increase or decrease were already occurring in precipitation trends across our study region in Arizona regardless of forest thinning and burning treatments. It was important to evaluate the temporal and spatial patterns of precipitation across our large study region, because precipitation varies across Arizona. The northern parts of the state at high elevations tend to have cooler climates with greater precipitation, whereas the southern part is warm throughout the year with lower amount of precipitation.

We used the Landsat 5 TM and Landsat 8 OLI surface reflectance (SR) image collections (LANDSAT/LT05/C01_SR and LANDSAT/L8/C01_SR collections,

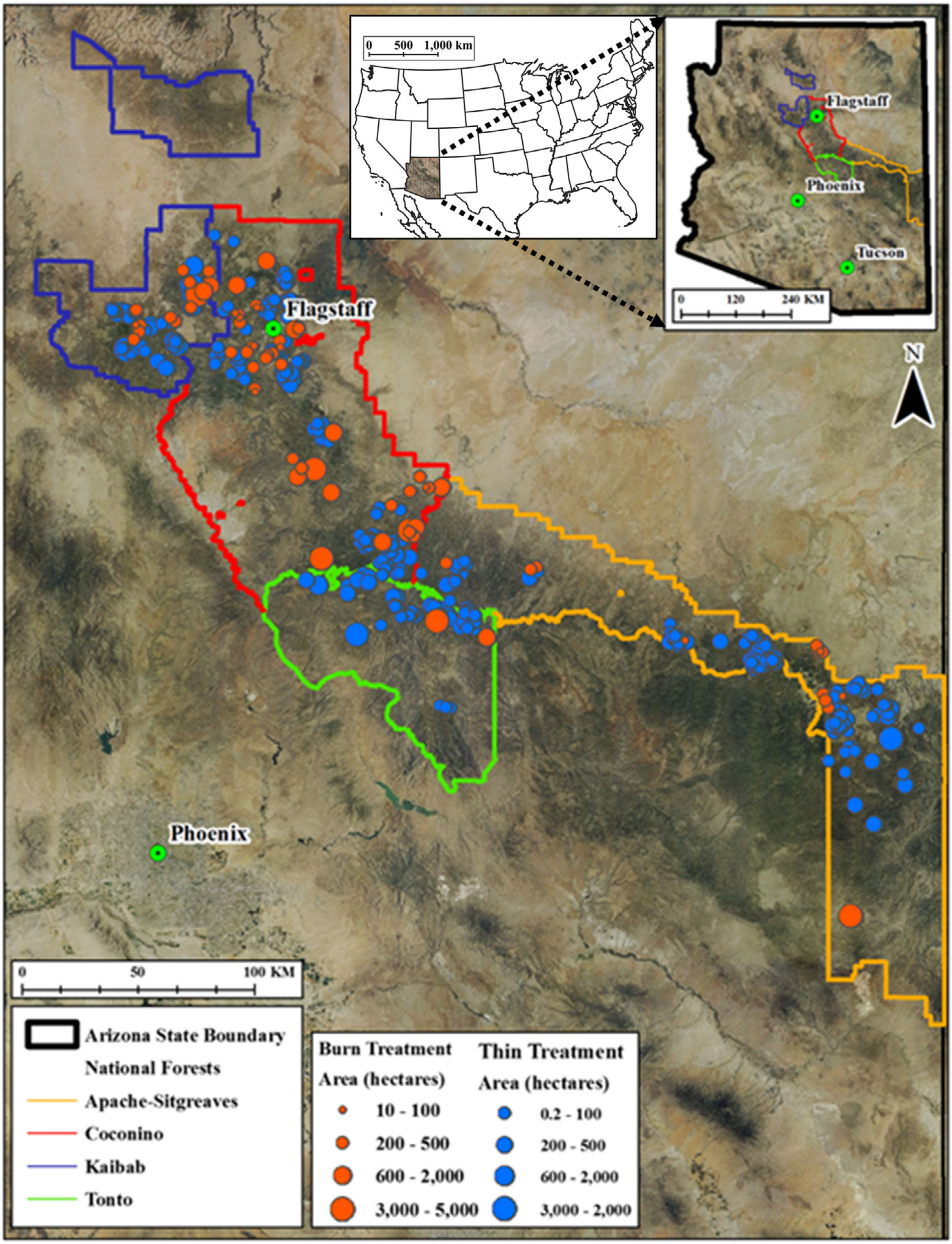

Figure 1. The Four Forest Restoration Initiative (4FRI) study region in Arizona, USA. 4FRI is the first and largest forest restoration effort in the US history. Since its launch in 2007, 4FRI has treated over 1200 polygon areas (Table1).

Table 1. Summary of the forest types and restoration treatments conducted over the study region since 2007.

Vegetation cover type	Total area (ha)	Total burned polygons	Total thinned polygons	Total burned area (ha)	Total thinned areas (ha)
Ponderosa pine	129,443	197	375	88,574	40,869
Mixed conifer	88,501	54	77	75,911	12,590
Pinyon-Juniper/Shrubs	218,556	219	306	165,472	53,094
TOTAL	436,510	467	758	329,957	106,553

respectively) from the GEE image archive for both time periods. Together, these collections included 4,426 Landsat images. The Landsat SR image collection in GEE were pre-processed with the Landsat ecosystem disturbance adaptive processing system (LEDAPS) algorithm (Masek et al., 2012). We further filtered the Landsat SR image collection to mask cloudy pixels. We also made the surface reflectance data from Landsat 8 more consistent with Landsat 5 data using the coefficients and regression models developed by Roy et al. (2017). In our analysis of pre-treatment and post-treatment period comparisons, it was important to consider and correct the sensor differences.

We divided each calendar year in the image collections into the following seasonal periods with the respective Julian dates: (1) Season 1 or pre-Monsoon spring: 91-180 (April 1-June 30), (2) Season 2 or summer Monsoon: 181-270 (July 1-September 30), (3) Season 3 or fall: 271-330 (October 1-November 30), and (4) Season 4 or winter: 331-90 (December 1-March 30). These seasonal periods reflect the expected relative changes in vegetation greenness and total moisture between different seasons. Annual precipitation in Arizona features a strong bimodal distribution with peaks in the winter and during the summer Monsoon season (Sankey et al., 2015). We, therefore, compared each season individually between the pre-treatment period versus the post-treatment period. For each season within each year, we produced a single mosaicked image by reducing the image collection to the 75th percentile NDVI values, which further eliminated cloud pixels that were not be eliminated in the surface reflectance by the LEDAPS algorithm (Massey et al., 2018).

Statistical Analysis

We calculated the following indices for each season within each time period using equations 1-3, respectively: 1) Normalized difference vegetation index (NDVI) (Rouse et al., 1972), 2) Normalized difference moisture index (NDMI), and 3) Normalized difference water index (NDWI) (McFeeters, 1996).

$$\mathrm{NDVI} = \frac{B4 - B3}{B4 + B3} \tag{1}$$

$$\mathrm{NDMI} = \frac{B4 - B5}{B4 + B5} \tag{2}$$

$$\mathrm{NDWI} = \frac{B2 - B4}{B2 + B4} \tag{3}$$

where B2, B3, B4, and B5 represent Landsat green, red, near-infrared, and shortwave infrared 1 bands, respectively. We chose NDVI in our arid and semi-arid forest ecosystems with relatively low biomass (Sankey et al., 2015; Theau et al., 2012) instead of enhanced vegetation index, for example, which might be appropriate in other forested ecosystems with large total biomass due to potential saturation (Huete et al., 2002; Huete et al., 1997). Our previous studies demonstrated that NDVI was sensitive to forest cover, density, and biomass reduction in Arizona forests as a result of thinning and burning (Sankey et al., 2017; Belmonte et al., 2019; Shin et al., 2018). NDMI has been commonly used to monitor forest ecosystem moisture and thus overall forest health and conditions (Goodwin et al., 2008; Simons-Legaard et al., 2016), while NDWI has been used as an indicator of water content and availability. We, therefore, use NDMI as a broad potential indicator of total ecosystem moisture including both vegetation and soil moisture content within pixels. We use NDWI as a potential, additional indicator of total ecosystem moisture availability. Since NDMI and NDWI leverage different spectral bands, they emphasize opposite trends in their values. We, therefore, use NDMI and NDWI in combination, since forest canopy moisture and water content estimates were an important objective in our study to infer forest resiliency to drought, once we estimated NDVI as an approximate indicator of forest canopy cover, density, biomass, and photosynthetic activity. In the uncharacteristically dense forests, thinning and burning treatments reduce forest density, biomass, and canopy cover. Thus, a reduced NDVI due to thinning and burning treatments would be expected to be associated with reduced forest evapotranspiration and, therefore, increased moisture content.

Next, we calculated the median NDVI, NDMI, and NDWI values of each season per year to summarize the index values and layer stacked the median images to create time-series datasets for each period. In addition, we calculated the mean of all median images of each index within each time period and for each treatment polygon. We then compared the temporal mean values to determine if NDVI, NDMI, and NDWI values had significantly changed between the two different periods and among the four different seasons. We used analysis of variance (ANOVA) tests with Tukey's multiple pair-wise comparisons to determine where significant differences were observed.

We examined the temporal trend in the median values of each seasonal NDVI, NDMI, and NDWI image stacks, and in the annual total precipitation time series datasets using a Mann–Kendall test over the pre-treatment period and the post-treatment period. The Mann–Kendall rank correlation trend test (MK test) identifies the magnitude and direction of monotonic trend within each pixel of the image time-series (Sankey et al., 2015). The MK tau coefficient (Eastman et al., 2009; Mann, 1945) ranges between −1 and 1, where negative values indicate a decreasing trend over time. Positive MK tau coefficients indicate an increasing trend and coefficients close to 0 indicate an absence of a trend in a pixel. The MK test also determines the statistical significance of the trend, when such directional trends are observed. We chose the MK test in this analysis for the following characteristics: 1) it is resistant to potential outliers in time-series data (Neeti & Eastman, 2011; Neeti et al., 2012), 2) it can be performed with small sample sizes (Yue & Wang, 2004), and 3) it does not require a normal distribution in time-series data (Neeti & Eastman, 2011). The MK test, however, requires sufficient dates in a time-series (at least 8 consecutive dates) to identify significant temporal trends in a dataset. We, therefore, included only the earlier treatment dates from 2007 to 2010 in the post-treatment period analysis and carefully chose 400 polygons among the 1,225 treated forest polygons.

Within each median index image stack, we estimated the proportion of area (in ha and in percent) with significantly increasing and decreasing trends and examined if the direction of the trend changed from the pre-treatment period to the post-treatment period. Furthermore, we estimated the mean proportion of area with significant trends for each treatment type post-treatment and compared the mean values between the two treatment types using ANOVA tests to determine which treatment types were associated with the significantly greater increases in post-treatment NDMI and NDWI. We also added as covariates the significant trends in total annual precipitation data described above and the forest vegetation cover types, because we expected that the responses might vary due to precipitation trends and by cover type.

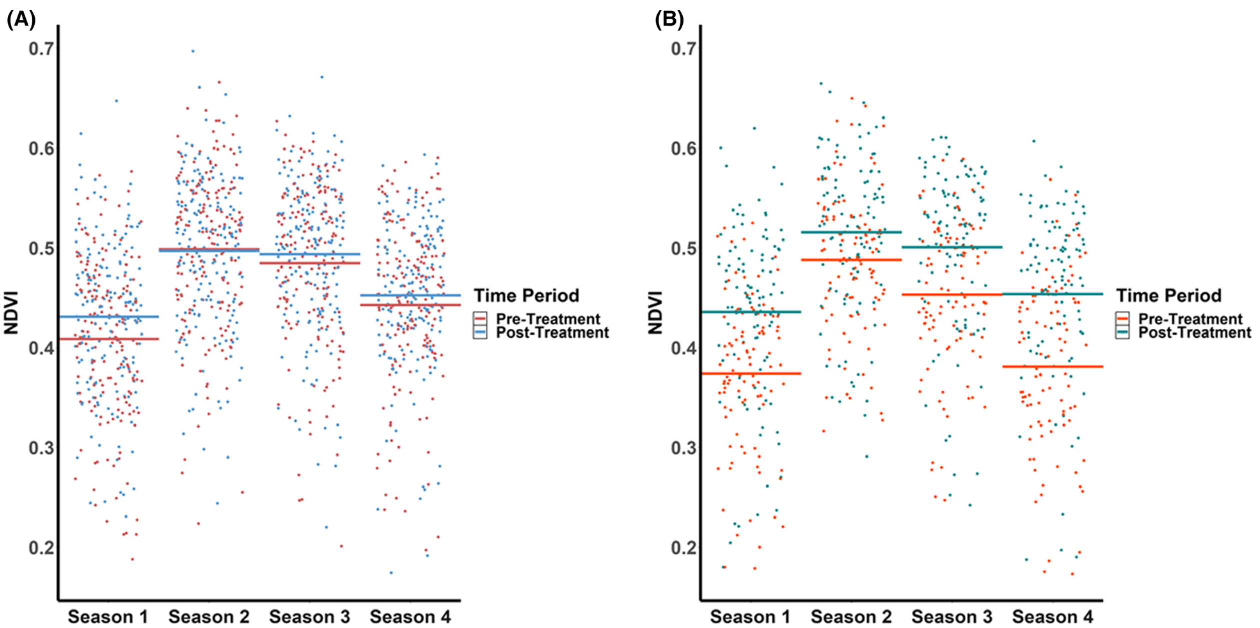

Figure 2. Comparisons of the mean NDVI values between the pre-treatment period (1990-2006) and post-treatment period (2007-2017). The annual cycle is divided into four seasons due to the annual precipitation distribution and phenological changes: Season 1 (April 1-June 30), Season 2 (July 1-September 30), Season 3 (October 1-November 30), and Season 4 (December 1-March 30). In thinned forests (Panel A), mean NDVI values were not significantly different for any of the seasons between the pre-treatment versus post-treatment periods. In burned forest polygons (Panel B), mean NDVI values were significantly greater following treatment for Seasons 1, 3, and 4 compared to the pre-treatment period (p-values <0.05).

Table 2. Mean index values compared between the pre-treatment versus post-treatment periods using an ANOVA test and Tukey's multiple pair-wise comparisons. Highlighted cells indicate significant differences ($p < 0.05$). The values shown are the calculated difference within each pair.

		NDVI: Burn	NDVI: Thin	NDMI: Burn	NDMI: Thin
Pre-Treatment versus Post-Treatment					
Season 1	Season 1	0.0618	0.0223	0.0833	0.0323
Season 2	Season 1	0.1415	0.0883	0.1474	0.0820
Season 3	Season 1	0.1267	0.0850	0.1817	0.1188
Season 4	Season 1	0.0795	0.0436	0.2512	0.1889
Season 1	Season 2	−0.0521	−0.0676	0.0163	−0.0234
Season 2	Season 2	0.0276	−0.0016	0.0804	0.0263
Season 3	Season 2	0.0129	−0.0049	0.1147	0.0631
Season 4	Season 2	−0.0343	−0.0463	0.1842	0.1332
Season 1	Season 3	−0.0173	−0.0536	0.0040	−0.0520
Season 2	Season 3	0.0624	0.0125	0.0681	−0.0023
Season 3	Season 3	0.0477	0.0092	0.1025	0.0345
Season 4	Season 3	0.0004	−0.0322	0.1720	0.1046
Season 1	Season 4	0.0546	−0.0120	−0.0206	−0.0896
Season 2	Season 4	0.1343	0.0541	0.0435	−0.0399
Season 3	Season 4	0.1195	0.0507	0.0779	−0.0030
Season 4	Season 4	0.0723	0.0094	0.1474	0.0671
Post Treatment versus Post Treatment					
Season 2	Season 1	0.1138	0.0899	0.0670	0.0557
Season 3	Season 1	0.0791	0.0758	0.0793	0.0843
Season 4	Season 1	0.0072	0.0343	0.1039	0.1218
Season 3	Season 2	−0.0348	−0.0141	0.0122	0.0286
Season 4	Season 2	−0.1066	−0.0557	0.0369	0.0661
Season 4	Season 3	−0.0719	−0.0416	0.0246	0.0376
Pre-Treatment versus Pre-Treatment					
Season 2	Season 1	0.0797	0.0660	0.0641	0.0497
Season 3	Season 1	0.0650	0.0627	0.0984	0.0866
Season 4	Season 1	0.0177	0.0213	0.1679	0.1566
Season 3	Season 2	−0.0147	−0.0033	0.0344	0.0368
Season 4	Season 2	−0.0620	−0.0447	0.1039	0.1069
Season 4	Season 3	−0.0472	−0.0414	0.0695	0.0701

Results

Annual precipitation and NDVI changes

In the pre-treatment period of 17 years, 394 951 ha or approximately 10% of the total area experienced significantly decreasing trend in annual total precipitation in central, central eastern, and northern parts of the state, whereas precipitation remained constant across the rest of the region. In the post-treatment period, the study region did not experience any statistically significant trend in annual total precipitation. Much of the forest restoration treatments have been conducted in ponderosa pine vegetation cover type comprising approximately 30% of the treated areas, whereas 20% and 25% of the treatments have occurred in mixed conifer and pinyon-juniper cover types, respectively.

Overall, thinning treatments did not significantly reduce the mean NDVI values (Figure 2, Panel A) for any of the four seasons (p-values >0.05 for all seasons). However, NDVI values were significantly different among different seasons as the forest phenology changed throughout the year (Table 2) as expected (Table 2). Similarly, burning treatments did not significantly reduce NDVI. Our results instead indicate that nearly all of the mean NDVI values were significantly greater in the post-treatment period (Figure 2, Panel B) in burned polygons. In particular, NDVI values from the pre-Monsoon season (season 1 (April-June)), fall season (season 3 (October-November)), and winter season (season 4 (December-March) were significantly greater compared to the pre-treatment mean NDVI values (Table 2).

When we examined the temporal trend in pre-treatment period NDVI, significantly declining trends were observed in the northern and eastern part of the study region, where it spatially overlapped with areas that experienced decreasing trends in precipitation in 1990-2006. While the decreasing trends in precipitation was a significant predictor variable associated with this pattern (p-value <0.001), it only explained a very small portion of the variability (R^2=0.04). Among the 12,000 ha burning treatments, approximately 4000 ha or 33% had significantly declining NDVI values in most seasons over the pre-treatment period, while a very small area (~200 ha) had a significantly increasing trend. No statistically significant temporal trend was observed in the rest of these polygons. Among the 96 000 ha thinning treatments, almost 50% (~46 000 ha) were already experiencing significantly decreasing NDVI trends prior to treatment, which largely occurred in the pre-Monsoon spring season, while only 1700 ha showed significantly increasing NDVI trends mostly observed in the summer Monsoon season.

When the temporal trends in post-treatment NDVI values were examined, 1,200-2552 ha or 10-20% of the burned forests had a significantly increasing trend in NDVI, although there was no significant trend in annual total precipitation. Notably, ~1300 ha had significantly increasing NDVI trend in the pre-Monsoon dry season, whereas the largest areas with the increasing trend is observed over the summer Monsoon season between July 1 and September 30. Only <1% of the burned areas showed significantly decreasing post-treatment NDVI, while the remaining areas showed no statistically significant trend. Burning treatments resulted in larger areas of significantly increasing NDVI compared to the thinning treatments (p-value <0.001). In the thinned polygons, 6800-14 930 ha showed significantly increasing NDVI trends in the post-treatment period, whereas <1% of the thinned area had significantly decreasing NDVI trend. Most notable significantly increasing trends were observed in the winter, fall, and the summer Monsoon seasons, respectively. The pre-Monsoon spring season had the smallest area of significantly increasing trend with 6800 ha.

NDMI changes and temporal trends

Our analysis of the thinning treatments indicated that post-treatment mean NDMI values were significantly greater compared to the pre-treatment mean NDMI values (Figure 3, Panel A). In particular, thinned forest polygons had significantly greater post-treatment NDMI values in pre-Monsoon spring (April-June), fall season (October-November), and winter season (December-March) (Table 2), from which we infer that total ecosystem moisture significantly increased following treatment. Similarly, the mean NDMI values in burned polygons were significantly greater in the post-treatment period compared to the pre-treatment period in all four seasons, when each season was compared individually (Figure 3, Panel B) (Table 2).

When we examined the temporal trend in pre-treatment NDMI values, significantly declining trends were observed in areas with significantly decreasing trends in annual total precipitation (R^2=0.1; p-value<0.001). A total of 1600-3150 ha or up to 30% of the burning treatment areas had a significantly decreasing trend in NDMI over the pre-treatment period (Figure 5), especially in the pre-Monsoon spring and winter seasons (Table 3). Up to 700 ha or <7% of the burning treatment areas had a significantly increasing trend in NDMI mostly observed in the summer Monsoon season (Table 3). Approximately 20 100-36 600 ha within the thinning treatment polygons were experiencing significantly decreasing pre-treatment NDMI trend (Figure 5) particularly in the pre-Monsoon season as well as the winter season. Approximately, 600-2740 ha of the thinning treatment polygons or only 6% of the total area experienced significantly increasing NDMI trend over the same time period, most of which was observed during the summer Monsoon season (Table 4).

When the temporal trend in NDMI over the post-treatment period was examined, much larger areas of significantly increasing trends were observed (Figure 5). Overall, treatment type was a significant predictor of increasing NDMI trend: burn treatments resulted in significantly larger areas of increasing NDMI trend (p-value=0.011). In contrast, treatment type was not a significant predictor of the decreasing NDMI trend post-treatment (p-value=0.09). Furthermore, vegetation type was a significant predictor variable in NDMI trends (p-value <0.001): ponderosa pine forests have significantly greater areas of increasing NDMI trend following treatment compared to other vegetation cover types. Among burning treatments, we observed a significantly decreasing trend in NDMI in only <1% of the areas, whereas we observed a significantly increasing trend across 670-1900 ha (Table 3). The thinned forest areas showed similar trends in the post-treatment period. Over 4300-11 000 ha or almost 10% of the thinned forests had significantly increasing NDMI trend following treatment, the largest of which were observed in the pre-Monsoon spring season (Table 4). In contrast, 1,900-2700 ha of the thinned areas had significantly decreasing NDMI trend, post-treatment, especially in the pre-Monsoon spring season and season was a significant predictor variable in ANOVA tests of decreasing NDMI trends (p-value<0.001), whereas vegetation cover type was not significant (p-value=0.136).

NDWI changes and temporal trends

When the pre-treatment period mean NDWI values were compared to the post-treatment period values, no significant changes were observed in the thinned forest polygons except for Season 2 (Figure 4, Panel A). In contrast, the post-treatment mean NDWI values were significantly lower in the burned forest polygons compared to the pre-

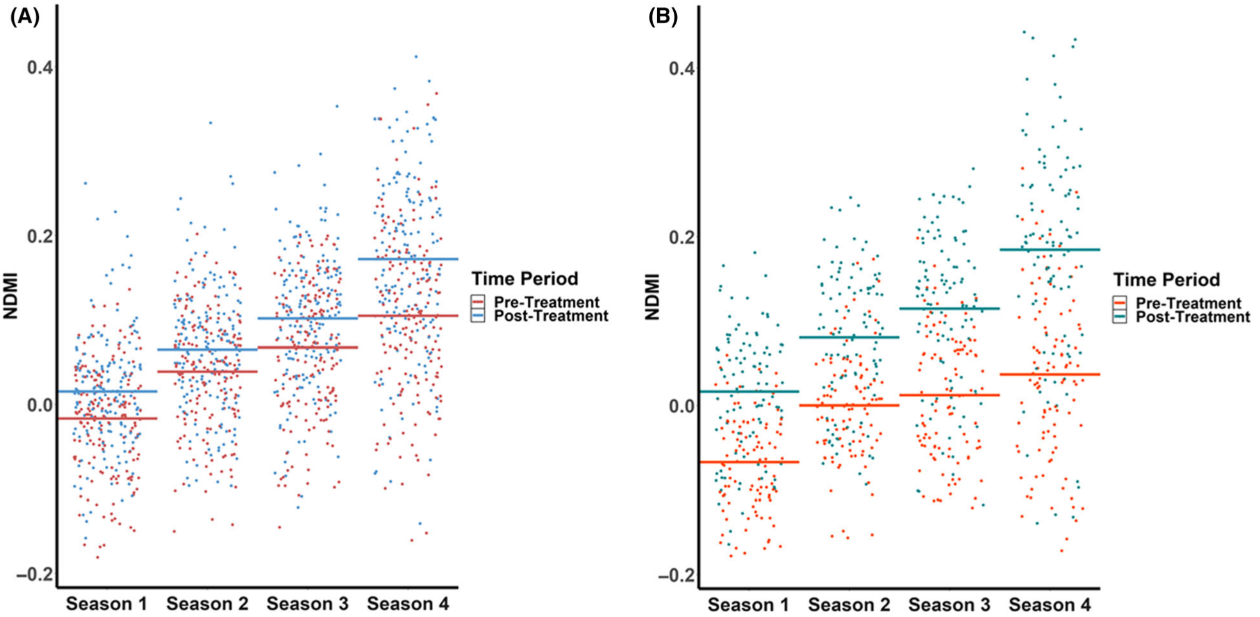

Figure 3. Comparisons of the mean NDMI values between the pre-treatment period (1990-2006) and post-treatment period (2007-2017). In thinned forests (Panel A), post-treatment mean NDMI values were significantly greater for all seasons, except Season 2, compared to the pre-treatment mean NDMI values. In burned forest polygons (Panel B), post-treatment mean NDMI values were significantly greater for all seasons compared to the pre-treatment period (p-values <0.05).

Table 3. Total areas (ha) within burning treatments with statistically significant trends observed over the pre-treatment and post-treatment time periods for each season: a) Season 1 (April 1-June 30), b) Season 2 (July 1-September 30), c) Season 3 (October 1-November 30), and d) Season 4 (December 1-March 30). These summaries only include forest polygons that received burning treatments in 2007-2010 (total area of 11,839 ha in 101 polygons), because the Mann–Kendall tau test requires more than eight consecutive years in the time-series analysis.

Indices	Season 1	Season 2	Season 3	Season 4
Decreasing trend in pre-treatment period NDMI	3151	2344	1608	3120
Increasing trend in pre-treatment period NDMI	571	580	701	51
Decreasing trend in post-treatment period NDMI	338	156	177	157
Increasing trend in post-treatment period NDMI	1900	1850	1608	670

Table 4. Total areas (ha) within burning treatments with statistically significant trends observed over the pre-treatment and post-treatment time periods for each season: (a) Season 1 (April 1-June 30), (b) Season 2 (July 1-September 30), (c) Season 3 (October 1-November 30), and d) Season 4 (December 1-March 30). These summaries only include forest polygons that received thinning treatments in 2007-2010 (total area of 96 402 ha in 170 polygons), because the Mann–Kendall tau test requires more than 8 consecutive years in the time-series analysis.

Indices	Season 1	Season 2	Season 3	Season 4
Decreasing trend in pre-treatment period NDMI	36,590	27,418	20,113	32 677
Increasing trend in pre-treatment period NDMI	2,476	2,712	3,709	681
Decreasing trend in post-treatment period NDMI	2,727	2,044	1,994	2650
Increasing trend in post-treatment period NDMI	1,127	8,531	9,985	4303

treatment mean values in all seasons, except for Season 2 (July 1-September 30) (Figure 4, Panel B).

When we examined the temporal trend in NDWI within the pre-treatment period, no significant temporal trend was observed over much of the treated areas. Only 1300 ha thinned area had a significantly decreasing trend in NDWI, whereas up to 3600 ha had a significantly increasing trend in NDWI mostly in the spring season. When we examined the temporal trend in NDWI post-treatment, no statistically significant trends were observed

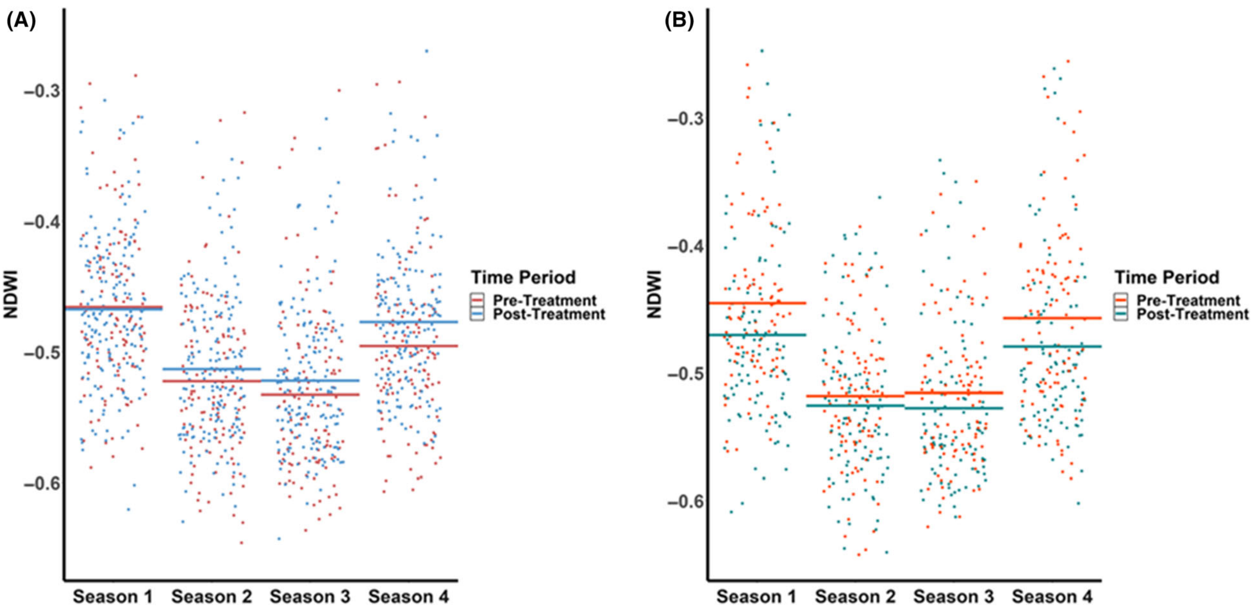

Figure 4. Comparisons of the mean NDWI values between the pre-treatment period (1990–2006) and post-treatment period (2007–2017). In thinned forests (Panel A), post-treatment mean NDWI values were not significantly different compared to the pre-treatment mean values for all seasons, except for Season 4. In burned forests (Panel B), post-treatment mean NDWI values were significantly lower for all seasons, except for Season 2, compared to the pre-treatment period (p-values <0.05).

in NDWI across much of the treated areas. But we observed a significantly increasing trend in 4400 ha and a decreasing trend in 3200 ha of the thinned areas. The size of areas with significant trends varied among the different seasons, although the largest hectares were consistently observed in the spring season.

Discussion

Our synthesis included over 4,400 Landsat 5 and 8 images on GEE. Classification and time-series analysis of such large datasets can be challenging, given the large image archive, large training datasets, and subsequent large computational demands, time, and funding required (Nemani et al., 2011; Gorelick et al., 2017), but GEE cloud-computing platform provides solutions to these challenges (Erickson, 2014; Gorelick et al., 2017). The computational efficiency of GEE combined with the complete archives of 40 years of pre-processed Landsat data and the GRIDMET surface meteorological dataset allowed the entire workflow and data merging within the same consistent environment. Several other studies have similarly produced Landsat-based analysis at regional and continental scales using GEE (Azzari and Lobell, 2017; Dong et al., 2015; Massey et al., 2018; Patel et al., 2015; Sankey et al., 2018; Simonetti et al., 2015; Padarian et al., 2015).

We first evaluated long-term trends in annual total precipitation across our study region and observed that much of the study region (up to 50% of the region in some seasons) was already experiencing a significantly decreasing trend in annual total precipitation prior to treatments. This is consistent with other studies that demonstrate predominantly drying trends that occurred across much of Arizona between 1980 and 2000 (Munson et al., 2016). We document with the Landsat image-derived moisture indices that the forest thinning and burning treatments have effectively targeted these areas and, in some cases, have altered the ecosystem response to the drying trends. While our analysis detected no significantly decreasing trends in precipitation since 2007, climate projection models predict increasing drought conditions with warmer temperatures and lower precipitation for the southwestern USA (Seager & Vecchi, 2010). Continued treatment activities will help reduce some of these projected impacts. Our synthesis and results (Figure 5) highlight where the treatment activities can continue to provide the most benefit for drought resiliency.

Forest changes

We provide the first synthesis of 4FRI (USDA, 2013), which spans a total area of 3.5 million ha. 4FRI's results and assessment of their progress and impacts are critical for other upcoming regional forest restoration efforts across the western USA (Allen et al., 2002; Cannon et al., 2018; Underhill et al., 2014), who will adopt similar

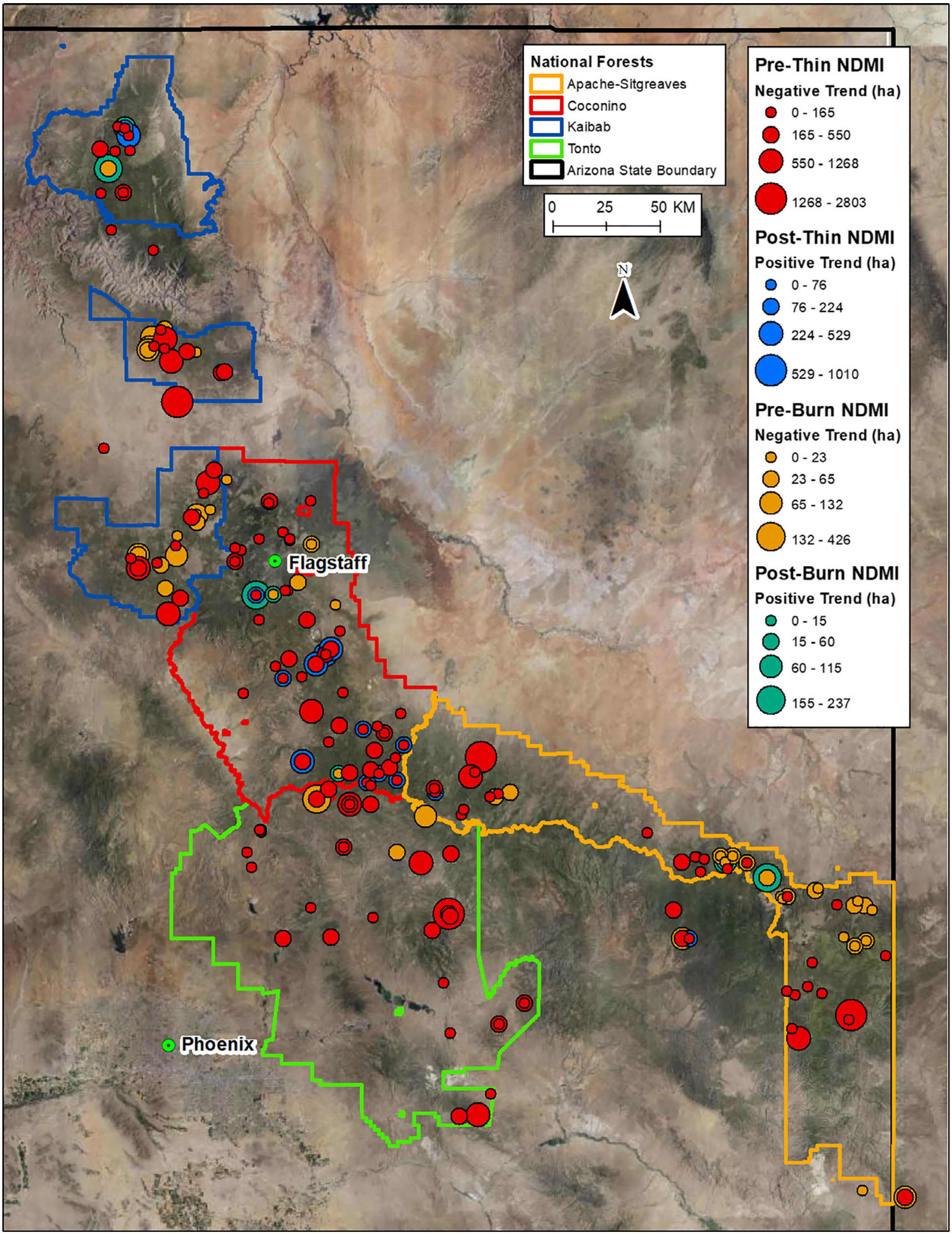

Figure 5. Spatial distribution of the pre-treatment and post-treatment trends in NDMI in the dry spring season, where significant trends in NDMI were observed in both time periods. In some treated areas, the statistically significant trends were reversed.

management strategies in other states. Since launching in 2007, 4FRI has treated over 1200 polygon areas within its boundary, using a variety of thinning and burning methods.

We use NDVI as an approximate indicator of forest canopy cover, density, biomass, greenness, and photosynthetic activity, and expected NDVI to change, when thinning and burning treatments were implemented across Arizona. We document that different treatments implemented have had varying effects on NDVI (Figure 3). Importantly, thinning treatments have resulted in different effects compared to the burning treatments and thinning treatments did not significantly reduce NDVI in each season. Previous remote sensing studies have documented significantly reduced NDVI following forest thinning (Belmonte et al., 2019; Sankey et al., 2015). Similarly, field-based and airborne observations have documented that forest thinning reduces canopy cover and tree density per unit area (Dickinson et al., 2016), and thus NDVI. However, our findings are not consistent with these patterns and this might be due to two specific factors. First, the thinning treatments were implemented in uncharacteristically dense stands that targeted the understory vegetation of dense, small diameter trees, rather than large overstory trees, to address the key concerns of wildfire risk. These forests were historically characterized with naturally open conditions (Covington & Moore, 1994) with a tree density of 142 trees per ha (Fule et al., 2009), but now have a tree density of 677 trees per ha due to fire exclusion and timber management (Cooper, 1960; Covington & Moore, 1994; Fule et al., 2009; Larson & Churchill, 2012; Savage et al., 1996). When 4FRI's thinning treatments substantially reduce such high density of small trees, there might still be a relatively high forest canopy cover due to the remaining trees (Roccaforte et al., 2010; Waltz et al., 2003). As a proxy of forest cover, density, biomass, and greenness, NDVI, therefore, might not be significantly reduced, when overstory trees are still remaining. Second, Landsat NDVI has been commonly documented to saturate at high tree canopy cover (Gitelson, 2003; Gitelson et al., 2003; Huete et al., 1997). Across our study region, we note that pre-treatment NDVI in the highest density forests with full canopy cover often peaked and plateaued at NDVI value of approximately 0.7. In these dense stands, forest canopy cover can remain high post-treatment within the 30 m pixels, despite overall tree density in the understory vegetation being substantially reduced. Furthermore, thinning treatment prescriptions target reduced basal area and the targets can be met by reducing overall tree density rather than canopy cover (Waltz et al., 2003). When canopy cover is not significantly reduced, despite basal area reductions, NDVI might not be change significantly.

We also document that burning treatments have resulted in significantly greater NDVI values for most seasons throughout the year. This is contrary to previous remote sensing studies that have documented significantly lower NDVI values following forest burning (Sankey et al., 2015) and field-based studies that commonly demonstrate lower tree canopy cover and density post-treatment (Fule et al., 2012; Lierop et al., 2015; Tuten et al., 2015). We note that there is one important distinction between our study and many previous studies and that is the time period at which our temporal analysis focused on. Our NDVI analysis compared the temporal mean NDVI values from the 1990–2006 period versus the temporal mean NDVI value from the 2007–2017 period. In addition, much of the study region experienced drought conditions in the pre-treatment period, where NDVI already had a significantly decreasing trend prior to the treatments. Unlike other studies that estimated NDVI immediately following fire or studies that compared one pre-treatment year versus one post-treatment year, we focus on the long-term mean change in NDVI. Furthermore, many of the burning treatments also target the understory vegetation of small trees. In locations, where there was low-severity burning, Landsat NDVI mean values might not change significantly, since overstory canopy cover and biomass might not change. Similar trends have been observed after restoration treatments in Colorado and was attributed to high residual tree density following treatments, especially compared to the historical forest conditions (Cannon et al., 2018). In addition, post-treatment NDVI might be similar to or greater than pre-treatment mean NDVI values due to increased understory vegetation biomass following treatment. Although forest restoration treatments likely reduced forest canopy cover, some understory vegetation cover and biomass significantly increase in Arizona and ponderosa pine forests following fire due to increased growth and influx of seedlings of both native and invasive species (Dore et al., 2012; McGlone et al., 2009; Vose & White, 1991). Such patterns likely contributed to the NDVI trends observed in our study, since the 30 m pixels of Landsat data are often mixed pixels consisting of both tree canopies and understory vegetation.

Treatment Effects on Forest Resiliency

We emphasize that many of the thinned and burned forest areas showed significantly decreasing trend in NDVI despite high canopy cover, density, and biomass prior to the treatments indicating low overall vigor, greenness, and photosynthetic activity. As discussed earlier, some of the significantly decreasing NDVI values occurred in areas that experienced drought conditions over the pre-treatment period especially in the pre-Monsoon spring season, the driest period in the region. More importantly, the predominantly decreasing trend in NDVI prior to treatment likely represent the overall health and the deteriorating conditions of the high-density forests. Our results indicate that treatments have either stabilized the declining NDVI trend or in some cases, especially with burning treatments, have reversed the declining NDVI trend. We document that areas that received controlled burning treatment have significantly greater NDVI post-treatment with greater vigor, greenness, and phohosynthetic activity. This is particularly encouraging, given that millions of forests across the southwestern USA are considered to be no longer healthy and vulnerable to catastrophic wildfire and insect outbreaks (Allen et al., 2002; Covington et al., 1997), and are slated for restoration treatments. The stable or the reversed trends in NDVI values post-treatment likely indicate that forest treatments have helped restore the vigor and natural fire behavior of low-severity burns as observed in numerous field-based studies (Fule et al., 2012; Waltz et al., 2014). Although not evident in NDVI values, thinning treatments and the resulting lower tree density likely also made the forests less vulnerable to insect-caused mortality, because high tree density is a primary factor associated with tree mortality caused by insects such as the bark beetle in Arizona (Negron et al., 2009). Continued management in treated areas can sustain the desired conditions in the coming decades through fire and timber management that is different than the policies implemented in the last century (Cooper, 1960; Larson & Churchill, 2012; Savage et al., 1996).

Measuring and quantifying ecosystem resiliency can be ambiguous and difficult, especially as shifts in climate occur (Côté & Darling, 2010; Holling, 1973; Ponce-Campos et al., 2013). Here we explicitly examined long-term trends in NDMI and NDWI, as broad representations of total ecosystem moisture availability including forest canopy water content or the total amount of water in the tree canopy foliage and soil (Chen et al., 2005; Jackson et al., 2004). We broadly interpret trends in these indices as potential indicators of forest canopy moisture status and water stress (Hunt et al., 2012; Wang et al., 2013). We, therefore, infer changes in ecosystem moisture and resiliency to drought, when these indices significantly change. Previous literature have documented that forest evapotranspiration and canopy interception of snow can collectively reduce the total ecosystem water budget (Barnes et al., 2016; Gray et al, 2002; Simonin et al., 2007; Zhang et al., 2001). Consequently, forest stands with high canopy cover and density would likely be more water-stressed due to high evapotranspiration and the reduced ecosystem water budget, especially in dry time periods as the available soil moisture is more readily transpired in and near denser stands (Gray et al., 2002). Forest thinning and burning would be expected to reduce such water stress by reducing tree density and subsequent evapotranspiration and snow interception. Taken together, these trends would lead to healthier forest ecosystems that are less vulnerable and more resilient towards climate-induced stresses including drought.

Our results of NDMI and NDWI trends indicate that forest restoration treatments have significantly altered the total ecosystem moisture status and have benefitted the water-stressed forests. For example, forest treatments have significantly increased NDMI (Figure 3). In particular, we emphasize that post-treatment mean NDMI values are significantly greater than pre-treatment values in the pre-Monsoon spring season, when forests in Arizona are especially dry and vulnerable to water stress and potential wildfire. During the winter period and extending into the warmer spring, Arizona forests predominantly use soil moisture originating from the snow as their main source of water (Kerhoulas et al., 2013). Our results highlight not only the importance of compounded seasonal moisture variability on long-term resiliency, but also corroborate the effects of using forest treatment as a method for contributing towards soil water accumulation (Feeney et al., 1998; McDowell et al., 2006; Skov et al., 2004). Our combined trends in all three indices, NDVI, NDMI, and NDWI, demonstrate that the forest restoration activities have resulted in significant changes in forest health and trends in forest condition. From these results, we infer that the restoration treatments have contributed toward improved forest resiliency to drought (Figure 5). While 4FRI's impacts have spatially varied across the region, our results in the NDMI trends illustrate where the greatest potential benefits are observed. These results have important implications for the continued forest restoration activities across the southwestern USA in the coming decades.

Scope and Limitations

Our synthesis demonstrates where forest restoration treatments have been conducted and how the treatments have impacted long-term vegetation index and moisture index trends post-treatment. Forest managers in similarly arid and semi-arid regions around the world can consider if our results can inform their forest restoration plans and strategies. Specifically, forested areas that are experiencing significantly drying trends might consider our results in efforts to slow down or potentially reverse the trends. The applicability of our methods in such scenarios and forest restoration monitoring are especially practical, given that all of our analysis was performed on GEE with the freely available algorithms and datasets covering the entire world.

We note that our results indicate that most of the forest restoration treatments in Arizona have been conducted in ponderosa pine, mixed conifer, and pinyon-juniper vegetation cover types. Therefore, many of our results in vegetation index and moisture index trends post-treatment might be limited to similar forest cover types in arid and semi-arid regions. Deciduous forests and ecosystems with many canopy layers, for example, might respond to similar restoration treatments differently, although long-term, post-treatment effects in such systems can still be similarly monitored on GEE using our methods.

Conclusion

Since 4FRI is the first large effort in the US history to focus on regional forest restoration, many important lessons can be learned and transferred to other states, who will similarly launch their restoration initiatives. Google Earth Engine cloud-computing platform enabled our synthesis of the spatial patterns and the long-term trends in NDMI, NDWI, NDVI, and annual total precipitation since 1990. We provide the first comprehensive assessment of the treatments and document where and how the treatments have been effective. Importantly, we demonstrate that some treatments have reduced forest vulnerability to drought conditions, and likely to wildfire risks and insect outbreaks, although treatment effects have spatially varied across the large region. Increasing analytical and computational capacities within Google Earth Engine will further enhance our continued monitoring of regional natural resource management.

References

Abatzoglou, J.T. (2012) Development of gridded surface meteorological data for ecological applications and modelling. *International Journal of Climatology*, https://doi.org/10.1002/joc.3413

Allen, C., Savage, M., Falk, D.A., Suckling, K.F., Swetnam, T.W., Schulke, T. et al. (2002) Ecological restoration of southwestern ponderosa pine ecosystems: a broad perspective. *Ecological Applications*, **12**(5), 1418–1433.

Andreadis, K.M., Storck, P. & Lettenmaier, D.P. (2009) Modeling snow accumulation and ablation processes in forested environments. *Water Resources Research*, **45**.

Asner, G., Nepstad, D., Cardinot, G. & Ray, D. (2004) Drought stress and carbon uptake in an Amazon forest measured with spaceborne imaging spectroscopy. *Proceedings of the National Academy of Sciences*, **101**, 6039–6044.

Baker, M.B. (1986) Effects of ponderosa pine treatments on water yield in Arizona. *Water Resources Research*, **22**(1), 67–73.

Barnes, M., Moran, S., Scott, R., Kolb, T., Ponce-Campos, G., Moore, D. et al. (2016) Vegetation productivity responds to sub-annual climate conditions across semiarid biomes. *Ecosphere*, **7**, 1–20.

Belmonte, A., Sankey, T., Biedermann, J., Bradford, J., Kolb, T. & Goetz, S. (2019) UAV-derived estimates of forest structure to inform ponderosa pine restoration. *Remote Sensing in Ecology and Conservation*, **6**, 181–197.

Briggs, J.S., Fornwalt, P.J. & Feinstein, J.A. (2017) Short-term ecological consequences of collaborative restoration treatments in ponderosa pine forests of Colorado. *Forest Ecology Management*, **395**, 69–80. https://doi.org/10.1016/j.foreco.2017.03.008

Chen, D., Huang, J. & Jackson, T.J. (2005) Vegetation water content estimation for corn and soybeans using spectral indices derived from MODIS near and short-wave infrared bands. *Remote Sensing of Environment*, **98**, 225–236.

Cooper, C.F. (1960) Changes in vegetation, structure, and growth of southwestern pine forests since white settlement. *Ecological Monographs*, **30**(2), 129–164.

Côté, I.M. & Darling, E.S. (2010) Rethinking ecosystem resilience in the face of climate change. *PLoS Biology*, **8**(7), e1000438. https://doi.org/10.1371/journal.pbio.1000438

Covington, W.W., Fule, P.Z., Moore, M.M., Hart, S.C., Kolb, T.E., Mast, J.N. et al. (1997) Restoring ecosystem health in ponderosa pine forests of the Southwest. *Journal of Forestry*, **95**(4), 23.

Covington, W.W. & Moore, M.M. (1994) Postsettlement changes in natural fire regimes and forest structure: ecological restoration of old-growth ponderosa pine forests. *Journal of Sustainable Forestry*, **2**(1–2), 153–181.

Dickinson, Y., Pelz, K., Giles, E. & Howie, J. (2016) Have we been successful? Monitoring horizontal forest complexity for forest restoration projects. *Restoration Ecology*, **24**, 8–17. https://doi.org/10.1111/rec.12291

Dong, J., Xiao, X., Menarguez, M.A., Zhang, G., Qin, Y., Thau, D. et al. (2015) Mapping paddy rice planting area in northeastern Asia with Landsat 8 images, phenology-based algorithm and Google Earth Engine. *Remote Sensing of Environment*, **185**, 142–154.

Eastman, R.J., Sangermano, F., Ghimire, B., Zhu, H., Chen, H., Neeti, N. et al. (2009) Seasonal trend analysis of image time series. *International Journal of Remote Sensing*, **30**, 2721–2726.

Erickson, T. (2014). Multi-source geospatial data analysis with Google Earth Engine. American Geophysical Union, Fall Meeting 2014, abstract #IN53E-05.

Feeney, S., Kolb, T., Covington, W. & Wagner, M. (1998) Influence of thinning and burning restoration treatments on presettlement ponderosa pines at the Gus Pearson Natural Area. *Canadian Journal of Forest Research*, **28**(9), 1295–1306. https://doi.org/10.1139/x98-103

Foley, J.A., DeFries, R., Asner, G.P., Barford, C., Bonan, G., Carpenter, S.R. et al. (2005) Global consequences of land use. *Science*, **309**(5734), 570–574.

Fule, P., Crouse, J., Roccaforte, J. & Kalies, E. (2012) Do thinning and/or burning treatments in western USA ponderosa or Jeffrey pine-dominated forests help restore natural fire behavior? *Forest Ecology and Management*, **269**, 68–81.

Fule, P., Korb, J. & Wu, R. (2009) Changes in forest structure of a mixed conifer forest, southwestern Colorado, USA. *Forest Ecology and Management*, **258**, 1200–1210.

Gitelson, A.A. (2003) Wide dynamic range vegetation index for remote quantification of biophysical characteristics of vegetation. *Journal of Plant Physiology*, **165**, 165–173.

Gitelson, A.A., Viña, A., Arkebauer, T.J., Rundquist, D.C., Keydan, G. & Leavitt, B. (2003) Remote estimation of leaf area index and green leaf biomass in maize canopies. *Geophysical Research Letters*, **30**(5), 1248.

Goodwin, N.R., Coops, N.C., Wulder, M.A., Gillanders, S., Schroeder, T.A. & Nelson, T. (2008) Estimation of insect dynamics using a temporal sequence of Landsat data. *Remote Sensing of Environment*, **112**, 3680–3689.

Gorelick, N., Hancher, M., Dixon, M., Ilyushchenko, S., Thau, D. & Moore, R. (2017) Google Earth Engine: Planetary-scale geospatial analysis for everyone. *Remote Sensing of Environment*, **202**, 18–27.

Gottfried, G.J. & Ffolliott, P.F. (1980) Evaluation of snowmelt lysimeters in an Arizona mixed conifer stand. *Hydrological and Water Resources in Arizona and Southwest*, **10**, 221–229.

Gray, A., Spies, T. & Easter, M. (2002) Microclimatic and soil moisture responses to gap formation in coastal Douglas-fir forests. *Canadian Journal of Forest Research*, **32**(2), 332–343. https://doi.org/10.1139/x01-200

Hancher, M. (2013) Planetary-scale geospatial data Analysis techniques in Google's Earth Engine platform. American Geophysical Union, Fall Meeting, abstract #IN52A-07.

Hansen, M.C., Potapov, P.V., Moore, R., Hancher, M., Turubanova, S.A., Tyukavina, A. et al. (2013) High-resolution global maps of 21st-century forest cover change. *Science*, **342**, 850–853.

Harpold, A.A., Biederman, J.A., Condon, K., Merino, M., Korgaonkar, Y., Nan, T. et al. (2014) Changes in snow accumulation and ablation following the Las Conchas Forest Fire, New Mexico, USA. *Ecohydrology*, **7**(2), 440–452.

Hidalgo, D.M., Oswalt, S.N. & Somanathan, E. (2015) Status and trends in global primary forest, protected areas, and areas designated for conservation of biodiversity from the Global Forest Resources Assessment 2015. *Forest Ecology and Management*, **352**, 68–77.

Holing, C.S. (1973) Resilience and stability of ecological systems. *Annual Review of Ecology and Systematics*, **4**, 1–23.

Huete, A., Didan, K., Miura, T., Rodriguez, E.P., Cao, X. & Ferreira, L.G. (2002) Overview of the radiometric and biophysical performance of the MODIS vegetation indices. *Remote Sensing of Environment*, **83**, 195–213.

Huete, A.R., Liu, H., van Leeuwen, W.J.D. (1997). The use of vegetation indices in forested regions: issues of linearity and saturation. IGARSS'97 1997 IEEE International Geoscience and Remote Sensing Symposium Proceedings. IEEE, Singapore: Remote Sensing - A Scientific Vision for Sustainable Development.

Hunt, R., Wang, L., Qu, J. & Hao, X. (2012) Remote sensing of fuel moisture content from canopy water indices and normalized dry matter index. *Journal of Applied Remote Sensing*, **6**(1), 061705–061705. https://doi.org/10.1117/1.jrs.6.061705

Jackson, T., Chen, D., Cosh, M., Li, F., Anderson, M., Walthall, C. et al. (2004) Vegetation water content mapping using Landsat data derived normalized difference water index for corn and soybeans. *Remote Sensing of Environment*, **92**(4), 475–482. https://doi.org/10.1016/j.rse.2003.10.021

Johansen, K., Phinn, S. & Taylor, M. (2015) Mapping woody vegetation clearing in Queensland, Australia from Landsat imagery using the Google Earth Engine. *Remote Sensing Applications: Society and Environment*, **1**, 36–49.

Keenan, R., Reams, G., Achard, F., Freitas, J., Grainger, A. & Lindquist, E. (2015) Dynamics of global forest area: Results from the FAO global forest resources assessment. *Forest Ecology and Management*, **352**, 9–20.

Kerhoulas, L., Kolb, T. & Koch, G. (2013) Tree size, stand density, and the source of water used across seasons by ponderosa pine in northern Arizona. *Forest Ecology and Management*, **289**, 425–433. https://doi.org/10.1016/j.foreco.2012.10.036

Köhl, M., Lasco, R., Cifuentes, M., Jonsson, Ö., Korhonen, K.T., Mundhenk, P. et al. (2015) Changes in forest production, biomass and carbon: Results from the 2015 UN FAO Global Forest Resource Assessment. *Forest Ecology and Management*, **352**, 21–34.

Larson, A.J. & Churchill, D. (2012) Tree spatial patterns in fire-frequent forests of western North America, including mechanisms of pattern formation and implications for designing fuel reduction and restoration treatments. *Forest Ecology and Management*, **267**, 74–92.

Mann, H.B. (1945) Nonparametric tests against trend. *Econometrica: Journal of the Econometric Society*, 245–259.

Massey, R., Sankey, T.T., Yadav, K., Congalton, R.G. & Tilton, J.C. (2018) Integrating cloud-based workflows in continental scale cropland extent classification. *Remote Sensing of Environment*, **219**, 162–179.

McDowell, N., Adams, H., Bailey, J., Hess, M. & Kolb, T. (2006) Homeostatic maintenance of ponderosa pine gas exchange in response to stand density changes. *Ecological Applications*, **16**(3), 1164–1182. 10.1890/1051-0761(2006)016[1164:hmoppg]2.0.co;2

McGlone, C., Springer, J. & Laughlin, D. (2009) Can pine forest restoration promote a diverse and abundant understory and simultaneously resist nonnative invasion? *Forest Ecology and Management*, **258**, 2638–2646.

Miura, S., Amacher, M., Hofer, T., San-Miguel-Ayanz, J., & Thackway, R. (2015) Protective functions and ecosystem services of global forests in the past quarter-century. *Forest Ecology and Management*, **352**, 35–46.

Moore, R.T. & Hansen, M.C. (2011) Google Earth Engine: a new cloud- computing platform for global-scale earth observation data and analysis. American Geophysical Union, Fall Meeting, abstract, IN43C-, 02.

Neeti, N. & Eastman, J.R. (2011) A contextual Mann-Kendall approach for the assessment of trend significance in image time series. *Transactions in GIS*, **15**, 599–611.

Neeti, N., Rogan, J., Christman, Z., Eastman, J.R., Millones, M., Schneider, L. et al. (2012) Mapping seasonal trends in vegetation using AVHRR-NDVI time series in the Yucatán Peninsula, Mexico. *Remote Sensing Letters*, **3**, 433–442.

Negron, J., McMillan, J., Anhold, J. & Coulson, D. (2009) Bark beetle-caused mortality in a drought-affected ponderosa pine landscape in Arizona, USA. *Forest Ecology and Management*, **257**, 1353–1362.

Ponce-Campos, G., Moran, M., Huete, A., Zhang, Y., Bresloff, C., Huxman, T. et al. (2013) Ecosystem resilience despite large-scale altered hydroclimatic conditions. *Nature*, **494** (7437), 349. https://doi.org/10.1038/nature11836

Rich, L.R. & Gottfried, G.J. (1976) Water yields resulting from treatments on the Workman Creek experimental watersheds in central Arizona. *Water Resources Research*, **12**(5), 1053–1060.

Roccaforte, J., Fulé, P. & Covington, W. (2010) Monitoring landscape-scale ponderosa pine restoration treatment implementation and effectiveness. *Restoration Ecology*, **18**(6), 820–833. https://doi.org/10.1111/j.1526-100x.2008.00508.x

Sankey, T. (2012) Decadal-scale aspen changes: evidence in remote sensing and tree ring data. *Applied Vegetation Science*, **15**, 84–98.

Sankey, T., Donald, J., McVay, J., Ashley, M., O'Donnell, F., Lopez, S.M. & et al. (2015) Multi-scale analysis of snow dynamics at the southern margin of the North American continental snow distribution. *Remote Sensing of Environment*, **169**, 307–319. https://doi.org/10.1016/j.rse.2015.08.028

Sankey, T., Massey, R., Yadav, K., Congalton, R. & Tilton, J. (2018) Post-socialist cropland changes and abandonment in Mongolia. *Land Degradation & Development*, **29**, 2808–2821.

Savage, M., Brown, P.M. & Feddema, J. (1996) The role of climate in a pine forest regeneration pulse in the southwestern United States. *Ecoscience*, **3**, 310–318.

Seager, R. & Vecchi, G.A. (2010) Greenhouse warming and the 21st century hydroclimate of southwestern North America. *Proceedings of the National Academy of Sciences USA*, **107**, 21277–21282.

Shin, P., Sankey, T., Moore, M. & Thode, A. (2018) Evaluating unmanned aerial vehicle images in estimating forest canopy fuels in a ponderosa pine stand. *Remote Sensing*, **10**, 1266–1277.

Simonetti, D., Simonetti, E., Szantoi, Z., Lupi, A. & Eva, H.D. (2015) First results from the phenology-based synthesis classifier using Landsat 8 imagery. *IEEE Geoscience and Remote Sensing Letters*, **12**, 1–5.

Simonin, K., Kolb, T.E., Montes-Helu, M. & Koch, G.W. (2007) The influence of thinning on components of stand water balance in a ponderosa pine forest stand during and after extreme drought. *Agricultural and Forest Meteorology*, **143**(3–4), 266–276.

Simons-Legaard, E.M., Harrison, D.J. & Legaard, K.R. (2016) Habitat monitoring and projections for Canada lynx: linking the Landsat archive with carnivore occurrence and prey density. *Journal of Applied Ecology*, **53**(4), 1260–1269. https://doi.org/10.1111/1365-2664.12611

Skov, K., Kolb, T. & Wallin, K. (2004) Tree size and drought affect ponderosa pine physiological response to thinning and burning treatments. *Forest Science*, **50**.

Theau, J., Weber, K. & Sankey, T. (2012) Multi-sensor analysis of vegetation indices in a semi-arid environment. *GIScience and Remote Sensing*, **47**, 260–275.

Trumbore, S., Brando, P. & Hartmann, H. (2015) Forest health and global change. *Science*, **349**(6250), 814–818.

Tuten, M., Sanchez-Meador, A. & Fule, P. (2015) Ecological restoration and fine-scale forest structure regulation in southwestern ponderosa pine forests. *Forest Ecology and Management*, **348**, 57–67.

Underhill, J.L., Dickinson, Y., Rudney, A. & Thinnes, J. (2014) Silviculture of the colorado front range landscape restoration initiative. *J. For.*, **112**, 484–493. https://doi.org/10.5849/jof.13-092

United States Department of Agriculture (USDA) (2013) *Draft Environmental Impact Statement for the Four-Forest Restoration Initiative*. Coconino County, Arizona: Coconino and Kaibab National Forests.

van Lierop, P., Lindquist, E., Sathyapala, S. & Franceschini, G. (2015) Global forest area disturbance from fire, insect pests, diseases and severe weather events. *Forest Ecology and Management*, **352**, 78–88.

Vose, J. & White, A. (1991) Biomass response mechanisms of understory species the first year after prescribed burning in an Arizona ponderosa-pine community. *Forest Ecology and Management*, **40**, 175–187.

Waltz, A., Fulé, P.Z., Covington, W.W. & Moore, M.M. (2003) Diversity in ponderosa pine forest structure following ecological restoration treatments. *Forest Science*, https://doi.org/10.1093/forestscience/49.6.885

Wang, L., Hunt, E.R., Qu, J.J., Hao, X. & Daughty, C.S.T. (2013) Remote sensing of fuel moisture content from ratios of narrow-band vegetation water and dry-matter indices. *Remote Sensing of Environment*, **129**, 103–110.

Yue, S. & Wang, C. (2004) The Mann-Kendall test modified by effective sample size to detect trend in serially correlated hydrological series. *Water Resources Management*, **18**, 201–218.

Zhang, L., Dawes, W.R. & Walker, G.R. (2001) Response of mean annual evapotranspiration to vegetation changes at catchment scale. *Water Resources Research*, **37**, 701–708.

